Neutron Halo in Heavy Nuclei from Antiproton Absorption

P. Lubiński, J. Jastrzębski,* A. Grochulska, A. Stolarz, and A. Trzcińska
Heavy Ion Laboratory, Warsaw University, PL-02-097 Warsaw, Poland

W. Kurcewicz*
Institute of Experimental Physics, Warsaw University, PL-00-681 Warsaw, Poland

F. J. Hartmann, W. Schmid, and T. von Egidy
Physik-Department, Technische Universität München, D-85747 Garching, Germany

J. Skalski, R. Smolańczuk, and S. Wycech
Soltan Institute for Nuclear Studies, PL-00-681 Warsaw, Poland

D. Hilscher, D. Polster, and H. Rossner
Hahn-Meitner-Institut, D-14109 Berlin, Germany
(Received 8 September 1994)

A new method to study the nuclear periphery using antiproton annihilation was applied to nine isotopes with mass numbers between 58 and 238. The method makes use of the detection of the radioactive annihilation products one unit lower in mass number than the target. A clear neutron halo effect, strongly correlated with the neutron binding energy, was observed in some nuclei. The experimental results are in qualitative agreement with calculations of proton and neutron densities at the nuclear periphery based on either a simple asymptotic density model or a more complex Hartree-Fock approach.

PACS numbers: 25.43.+t, 21.10.Gv, 36.10.–k

It is astonishing that even after decades of research the composition of the periphery of the atomic nucleus remains a puzzling problem. While recently discovered [1–3] large differences between the neutron and proton distribution in some light, neutron-rich nuclei are intensively studied [4], information on the nuclear periphery of heavy nuclei is not very abundant [5].

The situation where there is no substantial difference between rms radii of neutron and proton distributions, but a strong enhancement of the neutron density appears only at very large distances, presents a particular challenge for the experiment. This special "neutron halo" effect got its name more than 20 years ago [6]. This name shall also be adopted in this paper.

Experimental evidence accumulated up to now on the neutron halo in heavy nuclei is scarce [7–10] or even controversial [11,12]. A new and simple method to study the nuclear periphery was recently proposed [13]. It uses a radiochemical identification of the antiproton annihilation events in which the energy transferred to the nucleus is almost negligible.

The scenario of this study involves antiprotons slowed down in matter to less than 1 keV. Then an antiprotonic atom is formed by Auger electron emission. The antiproton cascades toward the nuclear surface, first emitting Auger electrons and later antiprotonic x rays. The antiprotonic cascade terminates far above the lowest Bohr orbit, when the antiproton encounters a nucleon at the nuclear surface and annihilates. For nuclei as heavy as ^{208}Pb the lowest accessible antiproton orbits have principal quantum number $n = 9$ or 10, the highest possible angular momentum, and radius of about 30 fm. Therefore, if an isospin signature of the annihilation is found, antiprotons could be used to probe the composition of the nuclear periphery. The total charge of pions emitted after annihilation was used as such a signature by Bugg *et al.* [10]. In the present work the identification of nuclear rather than mesonic products of the antiproton-nucleus interaction is employed for this purpose.

The method exploits the fact that for antiproton annihilations at distant orbits there is a large probability P_{miss} that all pions created during the annihilation miss the target nucleus (of mass number A_t, proton number Z_t, and neutron number N_t). As a result, a cold nucleus with mass $A_t - 1$ is produced. The ratio of the number of produced nuclei with one neutron less than N_t to the number of the nuclei with one proton less than Z_t is a function of the neutron and proton densities at distances r, where the product of two distributions, namely $P_{\mathrm{miss}}(r)$ and the antiproton absorption density $W(r)$, is sizable. If both $N_t - 1$ and $Z_t - 1$ products are radioactive, their production yield can easily be determined using gamma spectroscopy methods.

The experiment was performed using antiprotons from the Low Energy Antiproton Ring (LEAR) at CERN. The 200 MeV/c antiproton beam, delivered in the form of short (10–15 min) or long (80–90 min) duration "spills," was slowed down to about 7 MeV kinetic energy by a

plastic moderator after which individual antiprotons were counted using a scintillation detector. The antiproton counter and moderator were preceded by another detector, operating in anticoincidence and playing the role of the active diaphragm. A passive diaphragm was also used along the beam trajectory before and after the antiproton counter.

The target material consisted of foils of total thickness between 30 and 40 mg/cm^2 or of powder diluted in epoxy glue. Each target was placed between a few Al foils of known thicknesses (in total about 80 mg/cm^2 before and after the target). The Al thickness was selected in such a way that the 7 MeV antiprotons were stopped approximately in the middle of the target. However, as the target thickness was in general smaller than the antiproton range straggling, a fraction of the antiproton flux was stopped in the adjacent Al foils. Quantitatively this fraction was determined by detecting the ^{24}Na activity produced by antiprotons in these foils. Independently, we have established that 1000 $\overline{p}$ stopped in Al produce 21 ± 3 ^{24}Na nuclei.

Each target stack was bombarded by short or long spills (about 5×10^8 antiprotons). About 2 min after the end of irradiation the gamma ray counting was started and continued generally for a few months. HPGe detectors of about 20% and 60% efficiency and resolution slightly below 2 keV for the ^{60}Co 1333 keV transition were used. In some cases thin target foils (3–5 mg/cm^2) were also irradiated and counted using an x-ray HPGe detector. From the absolute intensities of the characteristic gamma ray lines, employing corrections for the radioactive decay during and after the irradiation, the number of $(Z_t, N_t - 1)$ and $(Z_t - 1, N_t)$ nuclei produced was deduced. For nonfissile targets the whole mass distribution (see, e.g., [14]) of the reaction products was also determined. In this way, by integrating the mass yield curve (and assuming that one reaction product is formed by one antiproton stopped in the target), the absolute number of antiprotons interacting with the target was confirmed.

Table I shows the results obtained for nine presently studied and evaluated targets. The last column of Table I gives the halo factor, defined in the same way as in Ref. [10]:

$$f_{\text{halo}}^{\text{periph}} = \frac{N(\overline{p}, n)\,\text{Im}(a_p) Z_t}{N(\overline{p}, p)\,\text{Im}(a_n) N_t},$$

where $N(\overline{p}, n)/N(\overline{p}, p)$ is the ratio of the produced $A_t - 1$ nuclei, and a_n and a_p are the $\overline{p}$-n and $\overline{p}$-p amplitudes [15] taken from Ref. [10]: $\text{Im}(a_n)/\text{Im}(a_p) = 0.63$. The ratio $\text{Im}(a_p)/\text{Im}(a_n)$ is supposed to give the ratio of $\overline{p}p$ and $\overline{p}n$ annihilation probabilities. Superscript "periph" accounts for the fact that $A_t - 1$ nuclei are produced in annihilations which are even more peripheral than the events seen in the experiment of Ref. [10], where all the annihilations contributed to the halo factor.

From Table I it can be seen that the $A_t - 1$ nuclei are produced in 10%–20% of the annihilation events and that the halo factor in measured cases varies at least by an order of magnitude. Its correlation with the neutron separation energy B_n is shown in Fig. 1. The observed scattering of the data points indicates that the neutron halo factor depends not only on B_n, but also on other properties of the nucleus and the atomic state in which the antiproton is captured. In particular, a strong $E2$ resonant mixing of the "upper" levels (and consequently a more distant annihilation site) is most probably responsible for the large values of the halo factor and $A_t - 1$ yield in ^{130}Te [16] and ^{176}Yb nuclei.

The significant differences in the halo factor for nuclei with a similar Coulomb barrier (as ^{96}Ru and ^{96}Zr or ^{144}Sm and ^{154}Sm) demonstrate that we go beyond a rather trivial effect of the proton wave function attenuation with this barrier here. Instead, the correlation of $f_{\text{halo}}^{\text{periph}}$ with the neutron separation energy, shown in Fig. 1, classifies the observed effect to the same category of phenomena (although with much smaller magnitude) as the neutron halo effects in light nuclei close to the neutron drip line [1–4].

TABLE I. Absolute production yield of $A_t - 1$ nuclei, their yield ratio, and peripheral halo factor.

Target	B_n (MeV)	Produced nuclei $\frac{N_t - 1}{1000\overline{p}}$	$\frac{Z_t - 1}{1000\overline{p}}$	$\frac{A_t - 1}{1000\overline{p}}$	$\frac{N(\overline{p}n)}{N(\overline{p}p)}$	$f_{\text{halo}}^{\text{periph}}$
$^{58}_{28}$Ni	12.2	46 ± 4	52 ± 7	98 ± 8	0.9 ± 0.1	1.3 ± 0.2
$^{96}_{40}$Zr	7.8	117 ± 17	44 ± 8	161 ± 22	2.6 ± 0.3	3.0 ± 0.4
$^{96}_{44}$Ru	10.7	50 ± 11	63 ± 13	113 ± 17	0.8 ± 0.2	1.1 ± 0.2
$^{130}_{52}$Te	8.4	149 ± 31	35 ± 7	184 ± 36	4.1 ± 0.4	4.3 ± 0.4
$^{144}_{62}$Sm	10.6	≤ 31	$^{\geq 86}_{\leq 137}$	117 ± 20	≤ 0.4	≤ 0.5
$^{154}_{62}$Sm	8.0	81 ± 15	40 ± 8	121 ± 20	2.0 ± 0.3	2.2 ± 0.4
$^{176}_{70}$Yb	6.9	211 ± 37	29 ± 11	241 ± 40	8.1 ± 0.7	8.4 ± 0.7
$^{232}_{90}$Th	6.4	81 ± 13	14 ± 2	95 ± 14	5.4 ± 0.8	5.4 ± 0.8
$^{238}_{92}$U	6.1	98 ± 8	16 ± 2	114 ± 9	6.0 ± 0.8	6.0 ± 0.8

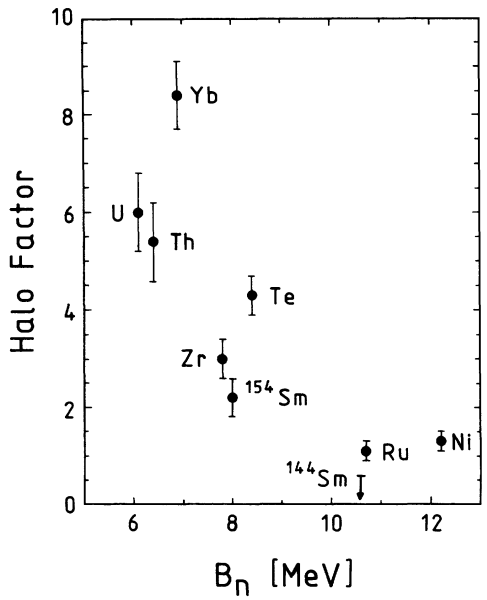

FIG. 1. Neutron halo factor (defined in the text) as a function of the target neutron separation energy B_n.

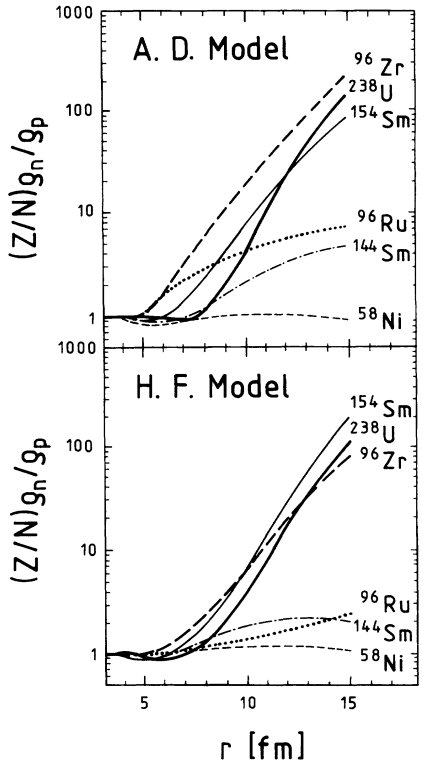

FIG. 2. Neutron to proton density ratio as a function of nuclear distance. Upper part: Asymptotic density model. Lower part: Hartree-Fock calculations.

In order to improve our understanding of the experimental results presented here, nuclear and atomic models have to be employed. In particular, with these models one should determine (a) densities of protons $\rho_p(r)$ and neutrons $\rho_n(r)$ at large nuclear distances; (b) antiproton absorption density with protons W_p and with neutrons W_n as a function of nuclear radius and atomic state quantum numbers; (c) $P_{\text{miss}}(r)$, i.e., the probability that the annihilation pions do not excite the target nucleus; and (d) fraction of the capture events occurring on deeply bound target nucleons and leading to the $A_t - 1$ nuclei with excitation energies above the neutron binding energy.

Calculations along these lines are presently in progress and a quantitative comparison of the experimental data with theory will be published soon. In the present paper we limit ourselves to the presentation of calculated neutron to proton density ratios at large nuclear distances. As shown below these ratios are in a qualitative agreement with the halo factors determined experimentally.

For a first guess a rather crude nuclear asymptotic density (AD) model was employed to understand the experimental results of Table I. Similar in principle to the Bethe and Siemens approach [17], the AD model used in the present work incorporates, however, a larger set of independent experimental data, treated as phenomenological input. For each analyzed target the charge density distribution in the surface area, the separation energies of proton and neutron, and the difference in rms radii of neutron and proton distribution were introduced. This model is expected to generate average level densities of the shell model, while it misses deformation, shell effects, and pairing correlations.

The last two effects are taken into account in a self-consistent mean field method which also generates a more reliable centrifugal barrier. In the present work we have used a code solving Hartree-Fock (HF) and Hartree-Fock-Bogoliubov (HFB) equations on the spatial mesh, with the effective Skyrme force SkP described in Ref. [18].

Figure 2 presents the calculated ratios of neutron to proton densities as a function of the nuclear distance for both models considered in this paper. Only HF results are presented, those of HFB being qualitatively similar. The most spectacular message of this figure is the theoretical confirmation of the increased relative neutron density in nuclear periphery for nuclei exhibiting a large halo factor in Table I. In spite of some differences between the results of the two approaches, both considered models agree qualitatively.

The preliminary calculations of antiproton absorption densities on proton, $W_p(r)$, on neutron, $W_n(r)$, and of the missing probability, $P_{\text{miss}}(r)$, were presented in Ref. [13]. These quantities are determined by antiproton and pion optical potentials, respectively. The antiprotonic potentials are based on the atomic x-ray data. The calculated P_{miss} follows in practice a black disk model, hence it may be determined by purely geometrical considerations. The validity of such a geometric approach is indicated by the pion multiplicity measurements [19,20]. The calculated

values of WP_{miss} show that the present method tests the nuclear surface composition at distances roughly equal to twice the root mean square radius. In order to be more precise in the above statement the influence of various selected $\overline{p}$ optical potentials on $W_n(r)$ and $W_p(r)$ should be investigated together with constraints imposed by the results of the present experiment.

In summary, a new method for the study of the nuclear periphery using antiproton absorption and nuclear spectroscopy techniques was applied to nine nuclei. In agreement with theoretical expectations a clear neutron halo signature was observed in nuclei with neutron binding energies smaller than about 9 MeV. The ensemble of the gathered experimental data may perhaps also be used to obtain more precise parameters of the antiproton-nucleus optical potential.

Fruitful discussions with Jan Błocki, Joseph Cugnon, Jacek Dobaczewski, Alexander Iljinov, Georg Riepe, and Władek Świątecki are gratefully appreciated. We also thank Dr. P. Maier-Komor and Mrs. K. Nacke for their invaluable help in target preparation. The competent cooperation of the LEAR staff during the irradiations and the support of ISOLDE and CERN Radioprotection Groups for our activation measurements is warmly acknowledged. This work was supported by Grants No. 2 0210 91 01 and No. 2P 302 140 04 from the Polish State Committee for Scientific Research and by the Joint Project No. POL-081.33 of Science and Technology cooperation between Germany and Poland.

*Present address: CERN, PPE Division, Isolde Group, Geneva, Switzerland.

[1] I. Tanihata, H. Hamagaki, O. Hashimoto, Y. Shida, N. Yoshikawa, K. Sugimoto, O. Yamakawa, T. Kobayashi, and N. Takahashi, Phys. Rev. Lett. **55**, 2676 (1985).

[2] P. G. Hansen and B. Jonson, Europhys. Lett. **4**, 409 (1987).

[3] P. G. Hansen, Nucl. Phys. News **1**, 21 (1991).

[4] B. Jonson, in "Proceedings of the 5th International Conference on Nucleus-Nucleus Collisions," Taormina, 1994 (to be published); Nucl. Phys. A (to be published).

[5] C. J. Batty, E. Friedman, H. J. Gils, and H. Rebel, Adv. Nucl. Phys. **19**, 1 (1989).

[6] J. A. Nolen, Jr. and J. P. Schiffer, Annu. Rev. Nucl. Sci. **19**, 471 (1969).

[7] D. H. Davis, S. P. Lovell, M. Csejthey-Barth, J. Sacton, G. Schorochoff, and M. O'Reilly, Nucl. Phys. **B1**, 434 (1967).

[8] H. J. Körner and J. P. Schiffer, Phys. Rev. Lett. **27**, 1457 (1971).

[9] E. H. S. Burhop, Nucl. Phys. **B44**, 445 (1972).

[10] W. M. Bugg, G. T. Condo, E. L. Hart, H. O. Cohn, and R. D. McCulloch, Phys. Rev. Lett. **31**, 475 (1973).

[11] S. Wycech, Nucl. Phys. **B28**, 541 (1971).

[12] W. J. Gerace, M. M. Sternheim, and J. F. Walker, Phys. Rev. Lett. **33**, 508 (1974).

[13] J. Jastrzębski, H. Daniel, T. von Egidy, A. Grabowska, Y. S. Kim, W. Kurcewicz, P. Lubiński, G. Riepe, W. Schmid, A. Stolarz, and S. Wycech, Nucl. Phys. **A558**, 405c (1993).

[14] J. Jastrzębski, W. Kurcewicz, P. Lubiński, A. Grabowska, A. Stolarz, H. Daniel, T. von Egidy, F. J. Hartmann, P. Hofmann, Y. S. Kim, A. S. Botvina, Ye. S. Golubeva, A. S. Iljinov, G. Riepe, and H. S. Plendl, Phys. Rev. C **47**, 216 (1993).

[15] M. Leon and R. Seki, Phys. Lett. **48B**, 173 (1974).

[16] S. Wycech, F. J. Hartmann, H. Daniel, W. Kanert, H. S. Plendl, T. von Egidy, J. J. Reidy, M. Nicholas, L. A. Redmond, H. Koch, A. Kreissl, H. Poth, and D. Rohmann, Nucl. Phys. **A561**, 607 (1993).

[17] H. A. Bethe and P. J. Siemens, Nucl. Phys. **B21**, 589 (1970).

[18] J. Dobaczewski, H. Flocard, and J. Treiner, Nucl. Phys. **A422**, 103 (1984).

[19] J. Cugnon, P. Deneye, and J. Vandermeulen, Nucl. Phys. **A500**, 701 (1989).

[20] D. Polster and D. Hilscher, in Second Biennial Workshop on Nucleon-Antinucleon Physics, Moscow, 1993 [J. Atomic Nuclei (to be published)].